J Incl Phenom Macrocycl Chem (2011) 71:103–111
DOI 10.1007/s10847-010-9907-0

ORIGINAL ARTICLE

Box–Behnken design for studying inclusion complexes of triglycerides and α-cyclodextrin: application to the heating protocol in molecular-dynamics simulations

Eduardo Walneide C. Almeida · Cleber P. A. Anconi · Willian Tássio G. Novato · Marcone A. L. De Oliveira · Wagner B. De Almeida · Hélio F. Dos Santos

Received: 13 July 2010 / Accepted: 19 November 2010 / Published online: 3 December 2010

Abstract In the present work, a Box–Behnken 3^4 design was applied to study inclusion complexes consisting of a saturated triglyceride with twelve carbons in each of the three side chains (TLG—trilaurylglyceride) and α-cyclodextrin (α-CD) in different TLG:α-CD stoichiometries: 1:1 (TLG@1.α-CD), 1:2 (TLG@2.α-CD) and 1:3 (TLG@3.α-CD). Four intrinsic variables commonly used to set up the heating protocol in the classical molecular-dynamics (MD) simulation were monitored: the heating ramp (W), the equilibrium time (E), the time step (S) and the dielectric constant of the medium (C). Based on the obtained responses, the most appropriate heating protocol and general aspects concerning the MD simulation of the host–guest supramolecular systems are discussed.

Keywords Molecular dynamics · Triglycerides · α-Cyclodextrin · Box–Behnken design

Introduction

Studies addressing inclusion compounds involving cyclodextrin (CD) are quite extensive. Since the fifties, when Freudenberg, Cramer and Plieninger [1] obtained a patent on such molecules, reports on the ability of CDs to form inclusion compounds with several targets have been described [2–8]. This property comes from the singular truncated cone-shape structure of the CD (Fig. 1a), which favors interactions with guest molecules, yielding host–guest inclusion complexes. In general, the guest molecules present hydrophobic characteristics that allow interaction with the hydrophobic cavity of CD and confer a certain stability to the inclusion compounds [2, 3, 9]. The importance of this process resides in the solubility of hydrophobic molecules that are insoluble in polar solvents and become soluble when included in the CD cavity due to the hydrophilic character of the external wall of the CD [10] (see Fig. 1a).

A class of molecules that presents hydrophobic properties and a strong appeal in the search of renewable energy sources is triglycerides (TGs) [11–17]. Studies involving inclusion complex of these molecules with cyclodextrins are scarce in the literature [11] and do not account for any potential applications of these systems in the development of biofuel-production technology. TGs have a structure based on glycerol, in which the hydrogen atoms of the alcoholic hydroxyls are substituted by carboxylate radicals (R) derived from fatty acids [12, 18] (Fig. 1b). The main sources of TG are animal fats and vegetable oils, the latter being the basis for the world production of biofuels.

Classical molecular-dynamics (MD) simulations are an important computational tool with several applications in the study of the host–guest-type compounds involving CD [19]. An important step towards the application of this

---

E. W. C. Almeida · W. T. G. Novato ·
M. A. L. De Oliveira · H. F. Dos Santos (✉)
Departamento de Química, ICE, Universidade Federal de Juiz de Fora, Campus Universitário, Juiz de Fora, MG 36036-330, Brazil
e-mail: helio.santos@ufjf.edu.br

C. P. A. Anconi
Departamento de Química, Universidade Federal de Lavras, Campus Universitário, Lavras, MG 37200-000, Brazil

W. B. De Almeida
Departamento de Química, ICEx, Universidade Federal de Minas Gerais, Campus Universitário, Belo Horizonte, MG 31270-901, Brazil

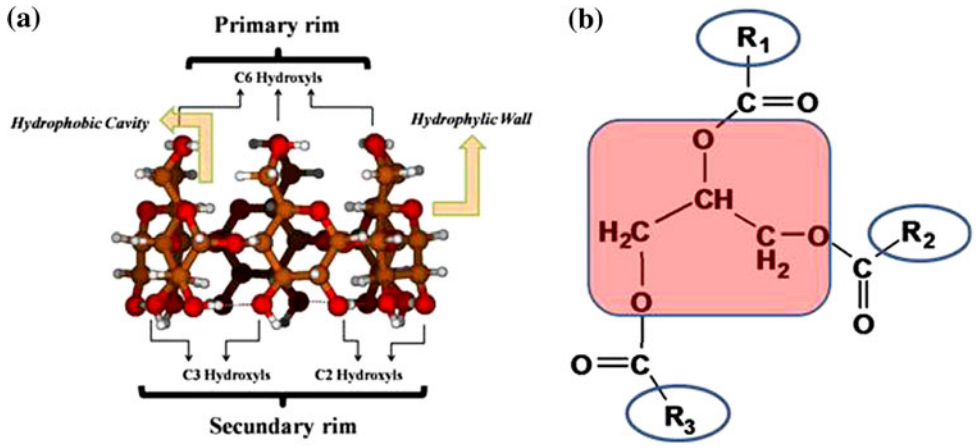

Fig. 1 **a** Structure of α-CD; **b** schematic representation of a triglyceride

methodology is optimization of the heating protocol, which is an artificial procedure required to warm the system to the simulation temperature (T = 298.15 K in the present work). This temperature can play a primary role in the stability of the equilibrium structures, mainly when non-covalently bound complexes are considered. Therefore, the study of the parameters defining the heating protocol is necessary to optimize the MD simulation and to provide reliable physical parameters at the end of the MD production phase. Four variables should be analyzed in the heating protocol: the heating ramp (W), the equilibrium time (E), the time step (S) and the dielectric constant of the medium (C) (see Fig. 2). The variables W and E, illustrated in Fig. 2, account for the heating intervals to which the system is submitted in the MD simulation and the time at which the system is left at a given temperature along the heating process, respectively. The former also comprises the time in which the temperature increases between two consecutive levels. The S variable is a mathematical parameter employed for the numeric integration of the equation of motion. The C variable allows the study of the behavior of a particular complex in distinct environments within the continuum-model formalism.

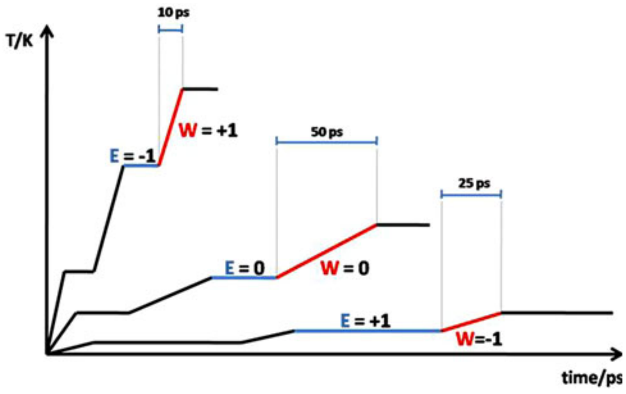

Fig. 2 Representative plot showing the distinct levels for the W and E variables employed in the Box–Behnken design

In the present work, we report on studies of MD simulation for 25 different heating protocols carefully planned using the Box–Behnken design [20]. Within our approach, three systems have been chosen, comprising the inclusion complexes formed by trilaurylglyceride (TLG, 12:0) and 1, 2 or 3 α-cyclodextrins, as depicted in Fig. 3. In addition, the most appropriate simulation protocol and some general aspects concerning theoretical MD investigations of host–guest supramolecular systems are discussed.

Theoretical methodology

The MD runs were carried out employing the AMBER* [21, 22] force field as implemented in the MacroModel® package [23]. The cutoff radii for van der Waals and coulombic electrostatic interactions were 8 and 20 Å, respectively. All C–H and O–H bond lengths were fixed using the SHAKE algorithm [24]. The solvent effect was accounted for within the generalized Born (GB/SA) formalism [25], which is a dielectric-continuum approach. The molecular models were built considering the inclusion process through the tail side of the α-CD cavity (narrower rim), with the initial distance between the primary hydroxyl groups of α-CD and the carbonyl groups of the TG being approximately 7.5–8.0 Å. The heating protocols were defined according to the values of the four basic variables shown in Table 1. The multivariate study was carried out with the aid of the Box–Behnken design for four variables and three levels, i.e., 3^4, labeled as high (+1), medium (0) and low (−1). The choice of the values for these variables was based on MD-simulation studies for CD associations [26] and its inclusion compounds [27]. The length of the production phase for all performed simulations, namely 25 assays, was 5,000 ps at a constant temperature of 298.15 K. The response monitored is referred to as the time factor (TF%) and is defined as the ratio of the time in which one CD unit leaves the TLG chain, the desinclusion

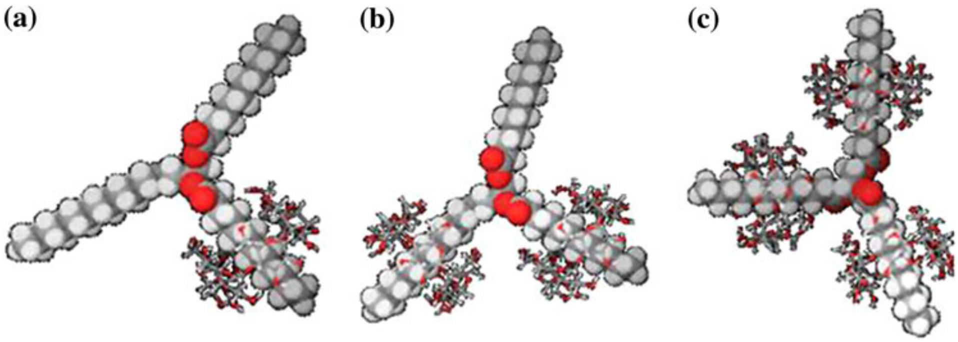

Fig. 3 Initial structures of the inclusion compounds studied: **a** 1:1 TLG@1.α-CD, **b** 1:2 TLG@2.α-CD and **c** 1:3 TLG@3.α-CD

instant (t_{desinc}), and the total length of the MD simulation including warming and production phases (t_{total}) via Eq. 1:

$$\text{TF\%} = \frac{t_{\text{desinc}}}{t_{\text{total}}} \times 100\% \tag{1}$$

The use of the TF% factor, the ratio between specific intervals, allows the comparison between distinct MD simulations, bearing in mind that distinct warming protocols imply in distinct total lengths (t_{total}). Therefore, the desinclusion process is presented in percentile terms to provide equivalent analyses of all assays. The identification of the exact instant of desinclusion, called the dethreading time, was based on the analysis of topological parameters established by the vectors $\overrightarrow{|\mu|}$ and $\overrightarrow{|D|}$ given in Fig. 4 and Eq. 2, where Ω is the angle between the oxygen ether atom O1, the last carbon of the TG chain and the oxygen ether atom O2.

$$\overrightarrow{|\mu|} = \overrightarrow{|D|} \cdot \operatorname{cotg}\left(\frac{\Omega}{2}\right) \tag{2}$$

Fundamentally, the desinclusion time is identified by a sudden increase in the norm of the vector between the center of the CDs shallow, truncated cone and the last carbon atom of the corresponding TLG chain. When the Ω angle tends to zero (which corresponds to desinclusion), the value of $\overrightarrow{|\mu|}$ tends to infinity because the cotangent becomes very large. This feature is also illustrated in Fig. 4 for a specific assay. According to the performed MD simulations, the desinclusion process occurs when the value of $\overrightarrow{|\mu|}$ is larger than 10 Å. The desinclusion is verified when $\overrightarrow{|\mu|}$ is at least twice the value of this limit, which prevents "artificial desinclusion events" involving the oscillation of the position of the CD along the TLG chain.

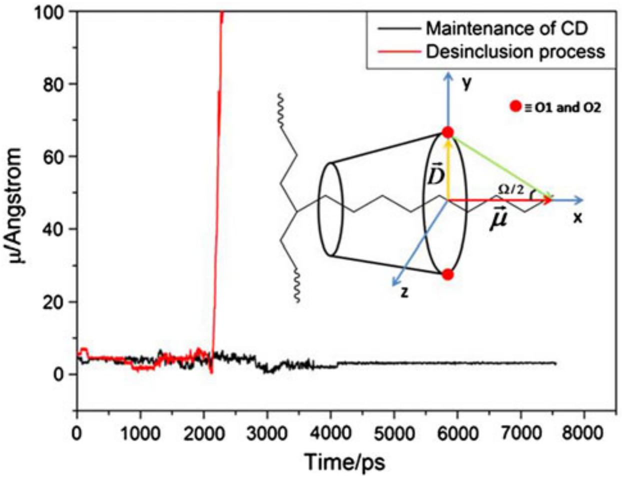

Fig. 4 Norm of $\vec{\mu}$ evaluated along a MD simulation. The instant of desinclusion is illustrated for assay 3

As previously stated, to define an appropriate protocol that maximizes TF%, a multivariate statistical analysis must be performed. In a system involving four significant independent variables, the mathematical relationship of the response to these variables can be approximated by a quadratic (second-degree) polynomial equation. Within our approach, in which the variables are W, E, S, C and the estimated response TF%, Eq. 3 can be used, in which β_0 is

Table 1 Levels of the independent variables applied for the Box–Behnken design

Level	Heating ramp (W) in K[a]	Equilibrium time (E) in ps	Time step (S) in fs	Dielectric constant (C)
−1	24.4	100	1.0	1
0	36.6	250	1.5	40.5
+1	48.9	400	2.0	80

[a] The values represent the average of difference along each distinct heating step as: 5/25/50/75/100/125/150/175/200/225/250/275/298.15, average of difference: 24.4 K (−1), 5/20/35/50/100/150/200/250/298.15, average of difference: 36.6 K (−0.004) and 5/50/100/150/200/250/298.15, average of difference: 48.9 K (1). The value in *parenthesis* represents the coded variable

a constant, β_1, β_2, β_3, and β_4 are linear coefficients, β_{12}, β_{13}, β_{14}, β_{23}, β_{24}, and β_{34} are interaction coefficients between the four factors and β_{11}, β_{22}, β_{33}, and β_{44} are the quadratic coefficients.

$$\begin{aligned}\mathrm{TF\%} =& \beta_0 + \beta_1\mathrm{W} + \beta_2\mathrm{E} + \beta_3\mathrm{S} + \beta_4\mathrm{C} \\ &+ \beta_{12}\mathrm{WE} + \beta_{13}\mathrm{WS} + \beta_{14}\mathrm{WC} + \beta_{23}\mathrm{ES} + \beta_{24}\mathrm{EC} \\ &+ \beta_{34}\mathrm{SC} + \beta_{11}\mathrm{W}^2 + \beta_{22}\mathrm{E}^2 + \beta_{33}\mathrm{S}^2 + \beta_{44}\mathrm{C}^2\end{aligned} \tag{3}$$

Equation 3 gives information about the effects of the individual variables and the interactions between them. The fitting of Eq. 3 was performed through the standard minimum-squares method and the critical values for the variables (maximum value of the response) were identified according to the literature [28, 29].

Results and discussion

The MD simulation performed with different heating protocols resulted, as expected, in distinct TF% values. For the complexes TLG@2.α-CD and TLG@3.α-CD, more than one TF% value was calculated for each assay, corresponding to distinct desinclusion events. However, because our main goal is to find a suitable heating protocol that maintains the integrity of the whole complex, only the first TF% deserves attention. Thus, the processes analyzed in the present study are given below:

TLG@1.α-CD → TLG + α-CD

TLG@2.α-CD → TLG@1.α-CD + α-CD

TLG@3.α-CD → TLG@2.α-CD + α-CD

All data concerning the tested protocols (coded and real values) and the responses are described in Table 2. The values in brackets correspond to assays in which the original host–guest system has been preserved along the heating protocol and, therefore, is found as an inclusion compound in the production period (5,000 ps for all simulations). According to the data in Table 2, most of the tested assays do not preserve the original host–guest structure up to the production phase, which is attested by a considerably small number of values reported in brackets. It is noticeable that most of the simulations result in desinclusion during the warming phase or the very beginning of the production period (data less than 10% in brackets have mean dethreading before 500 ps). It is also worth noting that the complexes constituted by two or three α-CD molecules are less stable than those with only one host molecule. The TF% values for the former are lower than 50% regardless of the heating protocol used. In Fig. 5, we plotted the TF% against the protocol number as quoted in Table 2. The relative heating time (heating time/total time) is also shown as a black continuous line. We note that the TF% responses closely follow the length of the heating phase, which means that the longer and slower the warming process, the larger the TF%. Nonetheless, there are some exceptions in Fig. 5 for which the TF% response is much larger than the relative heating time. These are more pronounced and frequent for a 1:1 stoichiometry, for which the assays 5, 6, 9 and 10 showed TF% > 80% and the assays 18, 19, 22 and 24 presented 50% < TF% < 60%. These assays should contain information concerning the best warming protocol.

The first step towards determining the best heating protocol is the calculation of the intrinsic effects of the four individual variables and the interactions between them, namely, the coefficients of Eq. 3. The obtained values of β_i, β_{ii} and β_{ij} are included in Table 3 and may give insight into the role of the variables in the final response in the MD simulations. In addition to the actual coefficients, the normalized values are also presented in parentheses in Table 3. These values are obtained from the fitting considering the coded variables, i.e., −1, 0 and +1, and directly reflect the weight of each independent variable in the final response. The normalized effects point to synergic (positive value) or antagonistic (negative value) contributions to the stability of the inclusion complexes. From these numbers, we note that the coefficients of the variables W (heating ramp) and E (equilibrium time) do not change significantly throughout the series of compounds analyzed, with the weight of E for TF% being slightly larger (~+20) than that of W (~−12). The sign analysis is also interesting and means that heating ramps with greater numbers of short temperature steps (W = −1) and larger equilibrium intervals (E = +1) improve the stability of the inclusion system (see Fig. 2). This result is somewhat expected once the potential energy change becomes subtle over the heating process. The dielectric constant of the medium (C) also plays a role to the response, mainly for the TLG@1.α-CD complex (−48.2). Interestingly, we observed that the weight of C decreases for complexes with two and three host molecules, as shown in Table 3 and Fig. 6a–c, which represents the E–C response surface (the most important variable according to Table 3). The interaction between the variables (cross-terms in Table 3) provides new information about the heating-protocol analysis, i.e., the possible synergistic or antagonistic relationship between the analyzed variables. In general, the effects are not very significant except for the variables WS and EC, whose values are larger than 10 for the TLG@1.α-CD process. In this case, both variables present a synergic effect for the stability of the complex, i.e., WS and EC > 0. For the other complexes, the crossed effects are less than 5 and are thus not discussed here. The effects of the quadratic variables (W^2, E^2, S^2 and C^2) are more pronounced and might be related to the weight of the variables in the rate

Table 2 Assays performed according to the 3^4 Box–Behnken design used to optimize the heating protocol of the MD simulation of TLG@n.α-CD inclusion complexes

Essay	Total time (ps)	W (K)	E (ps)	S (fs)	C	1st TF% 1:1	1st TF% 1:2	1st TF% 1:3
1	5,660	48.9 (+1)	100 (−1)	1.5 (0)	36 (−0.114)	15.0 [3.8]	7.9	9.8
2	6,320	24.4 (−1)	100 (−1)	1.5 (0)	36 (−0.114)	18.6	19.3	16.5
3	7,550	48.9 (+1)	400 (+1)	1.5 (0)	36 (−0.114)	28.4	28.2	28.6
4	10,100	24.4 (−1)	400 (+1)	1.5 (0)	36 (−0.114)	46.3	40.5	42.8
5	7,000	36.6 (+0.004)	200 (−0.333)	1.0 (−1)	1 (−1)	82.4 [75.3]	31.1 [3.5]	25.2
6	7,000	36.6 (+0.004)	200 (−0.333)	2.0 (+1)	1 (−1)	100 [100]	29.7 [1.6]	25.3
7	7,000	36.6 (+0.004)	200 (−0.333)	1.0 (−1)	80 (+1)	37.6 [12.7]	24.8	27.9
8	7,000	36.6 (+0.004)	200 (−0.333)	2.0 (+1)	80 (+1)	25.2	25.2	25.1
9	6,500	48.9 (+1)	200 (−0.333)	1.5 (0)	1 (−1)	100 [100]	21.9	21.4
10	8,000	24.4 (−1)	200 (−0.333)	1.5 (0)	1 (−1)	100 [100]	31.6	35.5
11	6,500	48.9 (+1)	200 (−0.333)	1.5 (0)	80 (+1)	21.1	19.6	19.6
12	8,000	24.4 (−1)	200 (−0.333)	1.5 (0)	80 (+1)	28.9	33.3	34.5
13	5,880	36.6 (+0.004)	100 (−1)	1.0 (−1)	36 (−0.114)	30.9 [18.7]	16.8 [2.1]	14.5
14	8,400	36.6 (+0.004)	400 (+1)	1.0 (−1)	36 (−0.114)	41.7 [2.1]	30.5	33.3
15	5,880	36.6 (+0.004)	100 (−1)	2.0 (+1)	36 (−0.114)	28.0 [15.4]	21.1 [7.2]	15.3 [0.3]
16	8,400	36.6 (+0.004)	400 (+1)	2.0 (+1)	36 (−0.114)	35.8	35.0	31.2
17	6,500	24.4 (−1)	200 (−0.333)	1.0 (−1)	36 (−0.114)	24.3 [1.6]	19.4	24.0 [1.3]
18	8,000	24.4 (−1)	200 (−0.333)	1.0 (−1)	36 (−0.114)	56.2 [29.9]	33.0	32.7
19	6,500	48.9 (+1)	200 (−0.333)	2.0 (+1)	36 (−0.114)	49.5 [34.3]	17.5	19.2
20	8,000	24.4 (−1)	200 (−0.333)	2.0 (+1)	36 (−0.114)	37.6	31.5	34.8
21	5,880	36.6 (+0.004)	100 (−1)	1.5 (0)	1 (−1)	34.9 [23.4]	25.0 [11.8]	12.8
22	8,400	36.6 (+0.004)	400 (+1)	1.5 (0)	1 (−1)	65.0 [41.3]	45.7 [8.8]	36.2
23	5,880	36.6 (+0.004)	100 (−1)	1.5 (0)	80 (+1)	12.2	16.7 [2.1]	11.7
24	8,400	36.6 (+0.004)	400 (+1)	1.5 (0)	80 (+1)	49.2 [14.6]	33.9	35.8
25	7,000	36.6 (+0.004)	200 (−0.333)	1.5 (0)	36 (−0.114)	27.0	35.1 [9.1]	25.8

The data for W, E, S and C factors correspond to the actual values employed in the Box–Behnken formalism. In *parentheses* the coded values are shown

The values in *brackets* correspond to TF% evaluated for the production time only (=5,000 ps for all MD simulations). These values are available only for the essays in which the complex survives up to the production phase

of change of TF%. Carefully looking at Table 3, we see that C^2 and E^2 are significant for TLG@1.α-CD and E^2 is significant for TLG@2.α-CD and TLG@3.α-CD. These results can be visualized in Fig. 6. For the 1:1 complex, the surface resembles a paraboloid, and for the 1:2 and 1:3 complexes the dependence of TF% on C variable is small and almost linear, indicating that the dielectric constant of the medium plays a primary role in the integrity of the TLG@1.α-CD inclusion complex, whereas the variable E is more important for the other forms.

A better interpretation of these models can be achieved after the evaluation of the critical values. The critical values for the variables are found by solving the system of equations comprising the following conditions:

$$\frac{\partial TF\%}{\partial W} = \frac{\partial TF\%}{\partial E} = \frac{\partial TF\%}{\partial S} = \frac{\partial TF\%}{\partial C} = 0 \qquad (4)$$

The results obtained are the optimized conditions and can be analyzed in terms of the response hypersurface. In our approach, the mathematical treatment has been carried out to determine the values that increase the response, TF%. The optimized MD-simulation conditions are reported in Table 4. As expected, the data in Table 4 are quite distinct for different stoichiometries but maintain the trend shown in Table 2 and Fig. 5. It is noticeable that, even when determining the optimal parameters for host–guest systems comprising more than one α-CD molecule, the predicted TF% value is lower than 50%. Therefore, for the TLG@2.α-CD and TLG@3.α-CD original systems, the dethreading occurs mostly during the heating phase, as clearly represented in Fig. 5. This feature, assuming the use of an appropriate force field, gives rise to a hypothesis to the fundamental question concerning MD simulations for host–guest complexes: are the studied systems unstable or does the desinclusion takes place because of an inadequate simulation heating protocol? Based on the first-TF% values (Table 2) and the predicted data included in Table 4 for the TLG@2.α-CD and TLG@3.α-CD systems, it can be stated

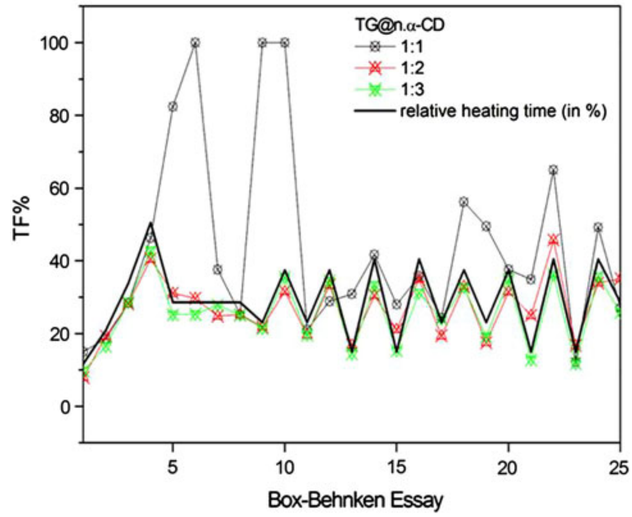

Fig. 5 Observed time factor (TF%) for the 25 assays analyzed. The relative heating time (heating time/total time) is also represented as a *continuous black line*

that such complexes are actually not stable within the approximations of the model.

Another intriguing aspect is related to the dielectric constant of the medium, which is the parameter that describes the solvent effect within the dielectric formalism. According to the data in Table 4, the optimal condition for TLG@1.α-CD and TLG@2.α-CD implies a dielectric constant equal to 1 (vacuum). Experimentally, host–guest complexes involving hydrophobic guests and CD are stable in aqueous media, and, therefore, a favorable condition should correspond to a dielectric constant near 80. In fact, the actual process is driven by the entropic contribution associated to the desolvation of the solute upon inclusion, which increases the solvent disorder around the substrate and, therefore, the entropy of the whole inclusion process. This effect, called the hydrophobic effect, cannot be accounted for by continuum solvation models [3]. Nonetheless, this apparent contradiction, which is a result of the theoretical approach used to include the solvent, does not invalidate the findings and conclusions drawn from the present study.

Another important feature for the stability of the complexes is related to the intrinsic structure of the guest. The saturated triglycerides are quite flexible molecules and tend to fold in gas phase at room temperature. This behavior is the same as that observed for poly(ethylene oxide) (PEO), which presents a folded form over a considerable temperature range and distinct solvents (C = 5 and C = 80) [25]. When the inclusion of these molecules takes place, the CD cavity forces the polymeric chain to acquire a partially linear arrangement, which should increase the potential energy, destabilizing the inclusion complex. In our recent study on carotenoids@β-CD inclusion complexes (unpublished results), a good direct relationship was established between the unfolding degree (the distance between the extremities) and the stabilization energy. For the TLG@2.α-CD and TLG@3.α-CD complexes studied here, the unfolding effect is expected to be more pronounced than for the 1:1 complex (TLG@1.α-CD), which might be related to the smaller values of TF% found for the formers. Actually, in our

Table 3 Mathematical coefficients obtained through the standard minimum-squares method for the three desinclusion processes investigated

Theoretical coefficients[a]	TLG@1.α-CD → TLG + α-CD	TLG@2.α-CD → TLG@1.α-CD + α-CD	TLG@3.α-CD → TLG@2.α-CD + α-CD
β_0	267.629 (28.7)	−80.8736 (38.7)	1.488 (30.1)
β_1/W	−6.2206 (−10.2)	2.6425 (−12.6)	−0.6121 (−13.1)
β_2/E	0.4021 (22.2)	0.236 (17.6)	0.2588 (21.3)
β_3/S	−174.0633 (−1.36)	56.1389 (1.06)	11.4184 (−1.53)
β_4/C	−1.6296 (−48.2)	0.1145 (−5.89)	0.0478 (−0.19)
β_{12}/WE	−0.002 (−7.49)	−7.09E−05 (−0.28)	−0.0008 (−2.84)
β_{13}/WS	1.7867 (21.9)	−0.0195 (−0.22)	−0.2838 (−3.47)
β_{14}/WC	−0.0037 (−3.41)	−0.002 (−1.94)	−0.0007 (−0.68)
β_{23}/ES	−0.0208 (−3.14)	0.0081 (1.22)	−0.0082 (−1.23)
β_{24}/EC	0.0012 (14.1)	−0.0002 (−2.93)	3.78E−05 (0.45)
β_{34}/SC	−0.3726 (−14.7)	0.0179 (0.71)	−0.0379 (−1.50)
β_{11}/W^2	0.0516 (15.4)	−0.0414 (−12.5)	0.0099 (2.87)
β_{22}/E^2	−0.0005 (−24.3)	−0.0004 (−15.9)	−0.0003 (−13.4)
β_{33}/S^2	42.5457 (21.3)	−19.0392 (−9.52)	0.341 (0.17)
β_{44}/C^2	0.0175 (54.6)	−0.001 (−3.16)	0.0003 (0.89)

The values in *parenthesis* represent the normalized effect of the coded variables

[a] The corresponding variable is included after *slash*. See Eq. 3

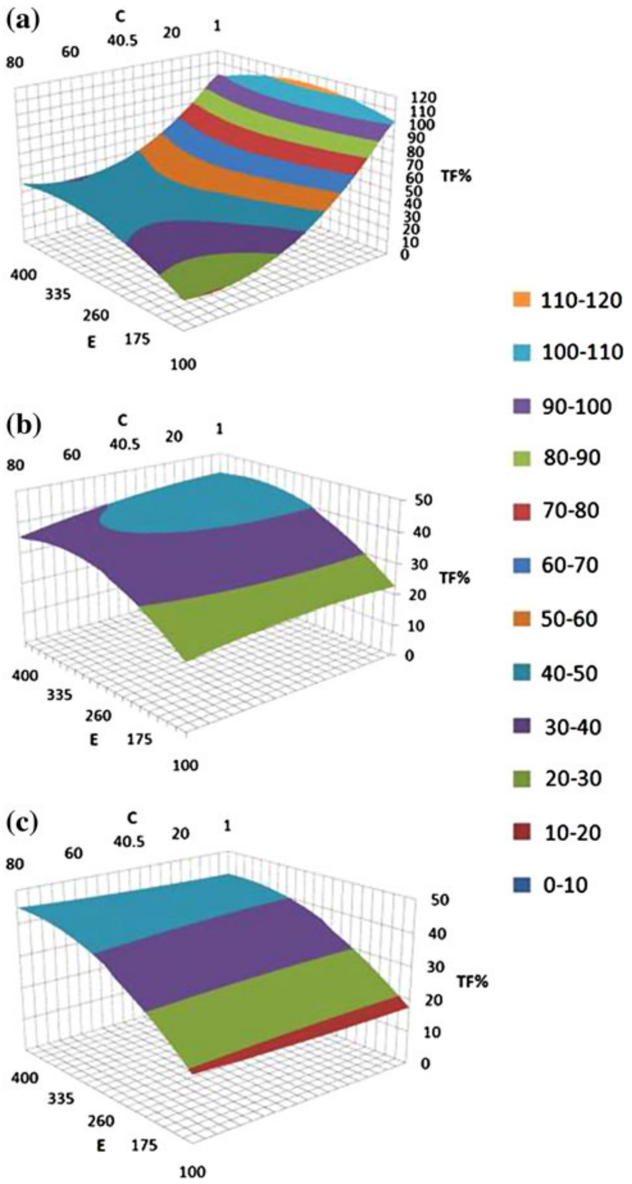

Fig. 6 Response surface for the first desinclusion processes of TLG@n.α-CD ($n = 1$, 2 and 3). Only the most important variables (E and C) are considered

approach, both effects have to be considered, i.e., the effect of the medium (represented by C) and the guest flexibility (not included in the present model). Therefore, based on the results obtained and the previous analysis, the subsequent discussion focus on the system originally possessing one α-CD (1:1) for which a stable complex is predicted for some heating protocols.

To understand and discuss the considerable amount of information obtained concerning the TF% values for the host–guest systems studied, focusing on the TLG@1.α-CD complex, two new MD simulations were performed. One simulation comprised the optimized conditions reported in Table 4, and the other comprised a set of conditions in which the C parameter corresponds to 80 (water). The latter condition has been evaluated by a random search for W, E and S variables performed to identify an acceptable theoretical response. In this search, the mathematical coefficients evaluated for the actual values (not coded) reported in Table 3 were employed. An acceptable response corresponds to a predicted TF% for which no desinclusion is expected along the heating phase. Therefore, the random search was performed to identify the higher theoretical TF% for which $C = 80$. The data obtained from both simulations and those concerning the assays 5, 6, 9 and 10 are reported in Table 5. As expected, for both tested conditions (optimized and acceptable), no desinclusion was identified along the heating protocol, as indicated by the values in brackets (TF% > 0). The TF% evaluated for the test with $C = 80$ is considerably small. In this simulation, the TLG@1.α-CD system was detected after the heating protocol but for a considerably small time in the production period. These results suggest that vacuum conditions ($C = 1$) produce more stable inclusion complexes at the end of the MD simulations, which is also attested by the analysis of the C value for the assays 5, 6 9 and 10 described in Table 5. In addition, we must realize that continuum models do not actually represent the solvent effect.

The Pareto chart of standardized effects (data not shown) attests that C and E are the most significant variables for the TLG@1.α-CD system. As discussed, $C = 1$ corresponds to the best choice in the present work, and the best choice for E corresponds to a value close to 200 ps. The comparison with the assays 5 and 6 indicates that $S = 2$ fs give rise to a better TF%, which is the same value for the optimized conditions. This result is interesting because a greater time step (S) will speed up a MD simulation with a predefined total length, decreasing the computational cost of the theoretical investigation. Finally, W being the less significant variable as attested by the Pareto chart and by comparison with the 9 and 10 assays, the choice of $W = 48.9$ K, suggested by the optimized parameters, seems to be an acceptable condition.

Conclusions

In the present work, a Box–Behnken 3^4 design was applied to optimize the main intrinsic variables controlling the heating phase of the molecular-dynamics (MD) simulation. The lifetime (TF%) of the inclusion complexes formed by α-cyclodextrin (α-CD) and trilaurylgliceride (TLG) was monitored and used as the response in the statistical analysis. The independent variables included in the model were the heating ramp (W), equilibrium time (E), time step (S) and the dielectric constant of the medium (C) in three

Table 4 Optimized variables of the heating protocol for the MD simulation of the TLG@n.α-CD inclusion complexes

MD variables	TLG@1.α-CD → TLG + α-CD[a]	TLG@2.α-CD → TLG@1.α-CD + α-CD[b]	TLG@3.α-CD → TLG@2.α-CD + α-CD[c]
W (K)	48.9	31.3	24.4
E (ps)	242	348	394
S (fs)	2	1.5	1
C	1	1	80
Predicted TF%	>100	44.4	44.8

The F_{reg} values are larger than the reference value of 2.92 at $\alpha = 0.05$ [30]

[a] $R^2 = 0.904$; $F_{reg} = 6.56$

[b] $R^2 = 0.956$; $F_{reg} = 13.2$

[c] $R^2 = 0.994$; $F_{reg} = 33.7$

Table 5 Independent variables and the corresponding responses for the best assays (5, 6, 9 and 10) and optimal conditions for C = 1 and C = 80

Quantities	TLG@1.α-CD → TLG + α-CD					
	Optmized conditions	Acceptable conditions	Essay 5	Essay 6	Essay 9	Essay 10
W (K)	48.9	24.4	36.6	36.6	48.9	24.4
E (ps)	242	400	200	200	200	200
S (fs)	2	1	1.0	2	1.5	1.5
C	1	80	1	1	1	1
Length	6,702 ps	10,100 ps	7,000 ps	7,000 ps	6,500	8,000
TF%	84.3 [79.0]	51.8 [2.6]	82.4 [75.3]	100 [100]	100 [100]	100 [100]

The results are for TLG@1.α-CD only

The values in *brackets* correspond to TF% evaluated for the production time only (5,000 ps)

levels coded as −1, 0 and +1. By analyzing the weight of the variables for the observed responses, we found that the dielectric constant (C) plays a primary role in the inclusion complex stability, with its effect being more pronounced for a 1:1 stoichiometry. In the case of the TLG@1.α-CD complex, the optimized variables used in the heating protocol were W = 48.9 K, E = 200 ps, S = 2 fs and C = 1, which led to TF% > 80%. For the other complexes, namely TLG@2.α-CD and TLG@3.α-CD, the lifetime (or time factor) was lower than 50% even when optimal values for the variables are used, suggesting that these systems are not at all stable. The main molecular reason for this instability may be the flexibility of the guest molecule, which is normally found in a folded form in the absence of the CD host. When included, the CD tends to force the guest structure to be linear and the potential energy then increases substantially, leading to the dethreading of the host–guest inclusion compound. It is expected that for less flexible molecules, such as unsaturated triglycerides, the inclusion complexes should be slightly more stable, and the optimal heating protocols established in the present study will be very useful for MD simulations. Furthermore, the optimized conditions (with exception of C) can probably be extended to simulations with an explicit solvent for which multivariate analysis would be certainly prohibitive due to the computational costs.

Acknowledgments The authors thank the Conselho Nacional de Desenvolvimento Científico (CNPq—479682/2008-9) for research concessions and for financial support and Fundação de Amparo à Pesquisa do Estado de Minas Gerais (FAPEMIG—CEX—APQ-00498-08) for the fomentation.

References

1. Loftsson, T., Duchêne, D.: Cyclodextrins and their pharmaceuticals applications. Int. J. Pharm. **329**, 1–11 (2007). doi:10.1016/j.ijpharm.2006.10.044
2. Connors, K.A.: The stability of cyclodextrin complexes in solution. Chem. Rev. **97**, 1325–1357 (1997). doi:10.1021/cr960371r
3. Szejtli, J.: Introduction and general overview of cyclodextrin chemistry. Chem. Rev. **98**, 1743–1754 (1998). doi:10.1021/cr970022c
4. Schneider, H.J., Hacket, F., Rüdiger, V., Ikeda, H.: NMR studies of cyclodextrins and cyclodextrin complexes. Chem. Rev. **98**, 1755–1785 (1998). doi:10.1021/cr970019t
5. Rekharsky, M.V., Inoue, Y.: Complexation thermodynamics of cyclodextrins. Chem. Rev. **98**, 1875–1918 (1998). doi:10.1021/cr970015o
6. Wenz, G., Han, B.H., Muller, A.: Cyclodextrin rotaxanes and polyrotaxanes. Chem. Rev. **106**(3), 782–817 (2006)

7. Uekama, K., Hirayama, F., Irie, T.: Cyclodextrin drug carrier systems. Chem. Rev. **98**, 2045–2076 (1998). doi:10.1021/cr970025p
8. Venturini, C.D.G., Nicolini, J., Machado, C., Machado, V.G.: Propriedades e aplicações recentes de ciclodextrinas. Quim. Nova **31**, 360–368 (2008)
9. Anconi, C.P.A., Nascimento, C.S., De Almeida, W.B., Dos Santos, H.F.: Theoretical study of α-CD based [3]pseudorotaxanes: the role played by threadlike polymer on the stability of cyclodextrin dimers. J. Braz. Chem. Soc. **19**, 1033–1040 (2008)
10. Easton, C.J., Lincoln, S.F.: Modified Cyclodextrins—Scaffolds and Templates for Supramolecular Chemistry. Imperial College Press, London (1999)
11. Kolossváry, G.J., Kolossváry, I.: Molecular dynamics simulation of cyclodextrin inclusion complexes in enzymatic lipid hydrolysis. Biotechnol. Lett. **18**, 440–444 (1996). doi:10.1007/BF00143467
12. Schuchardt, U., Sercheli, R., Vargas, R.M.: Transesterification of vegetable oils: a review. J. Braz. Chem. Soc. **9**, 199–210 (1998)
13. Ma, F., Hanna, M.A.: Biodiesel production: a review. Bioresour. Technol. **70**, 1–15 (1999). doi:10.1016/S0960-8524(99)00025-5
14. Altin, R., Çentikaya, S., Yücesu, H.S.: The potential of using vegetable oil fuels as fuel for diesel engines. Energy Convers. Manag. **42**, 529–538 (2001). doi:10.1016/S0196-8904(00)00080-7
15. Pousa, G.P.A.G., Santos, A.L.F., Suarez, P.A.Z.: History and policy of biodiesel in Brazil. Energy Policy **35**, 5393–5398 (2007). doi:10.1016/j.enpol.2007.05.010
16. Demirbas, A.: Progress and recent trends in biofuels. Prog. Energy Combust. Sci. **33**, 1–18 (2007). doi:10.1016/j.pecs.2006.06.001
17. Demirbas, A.: Biofuels sources, biofuel policy, biofuel economy and global biofuel projections. Energy Convers. Manag. **49**, 2106–2116 (2008). doi:10.1016/j.enconman.2008.02.020
18. Geris, R., Dos Santos, N.A.C., Amaral, B.A., Maia, I.D.S., Castro, V.D., Carvalho, J.R.M.: Biodiesel de soja—reação de transesterificação para aulas práticas de química orgânica. Quim. Nova **30**, 1369–1373 (2007)
19. Lipkowitz, K.B.: Applications of computational chemistry to the study of cyclodextrins. Chem. Rev. **98**, 1829–1874 (1998). doi:10.1021/cr9700179
20. Ferreira, S.L.C., Bruns, R.E., Ferreira, H.S., Matos, G.D., David, J.M., Brandão, G.C., Da Silva, E.G.P., Portugal, L.A., Dos Reis, P.S., Souza, A.S., Dos Santos, W.N.L.: Box–Behnken design: an alternative for the optimization of analytical methods. Anal. Chim. Acta **597**, 179–186 (2007). doi:10.1016/j.aca.2007.07.011
21. Weiner, S.J., Kollman, P.A., Case, D.A., Singh, U.C., Ghio, C., Alagona, G., Profeta Jr., S., Weiner, P.: A new force field for molecular mechanical simulation of nucleic acids and proteins. J. Am. Chem. Soc. **106**, 765–784 (1984). doi:10.1021/ja00315a051
22. Cornell, W.D., Cieplak, P., Bayly, C.I., Gould, I.R., Merz Jr., K.M., Ferguson, D.M., Spellmeyer, D.C., Fox, T., Caldwell, J.W., Kollman, P.A.: A second generation force field for the simulation of proteins, nucleic acids, and organic molecules. J. Am. Chem. Soc. **117**, 5179 (1995). doi:10.1021/ja00124a002
23. Mohamadi, F., Richards, N.G.J., Guida, W.C., Liskamp, R., Lipton, M., Caufield, C., Chang, G., Hendrickson, T., Still, W.C.: Macromodel—an integrated software system for modelling organic and bioorganic molecules using molecular mechanics. J. Comput. Chem. **11**, 440–467 (1990). doi:10.1002/jcc.540110405
24. Ryckaert, J.P.: Special geometrical constraints in the molecular-dynamics of chain molecules. Mol. Phys. **55**, 549–556 (1985)
25. Ferreira, B.A., Dos Santos, H.F., Bernardes, A.T., Silva, G.G., De Almeida, W.B.: Theoretical study of solvent and temperature effects on the behaviour of poly(ethylene oxide) (PEO). Chem. Phys. Lett. **307**, 95–101 (1999). doi:10.1016/S0009-2614(99)00501-1
26. Bonnet, P., Jaime, C., Morin-Allory, L.: α-, β-, and γ-cyclodextrin dimers. Molecular modeling studies by molecular mechanics and molecular dynamics simulations. J. Org. Chem. **66**, 689–692 (2001). doi:10.1021/jo0008284
27. Anconi, C.P.A., Nascimento, C.S., De Almeida, W.B., Dos Santos, H.F.: Structure and stability of $(\alpha\text{-CD})_3$ aggregate and OEG@$(\alpha\text{-CD})_3$3 pseudorotaxane in aqueous solution: a molecular dynamics study. J. Phys. Chem. B **113**, 9762–9769 (2009)
28. Dos Santos, W.L., Dos Santos, C.M.M., Costa, J.L.O., Andrade, H.M.C., Ferreira, S.L.C.: Multivariate optimization and validation studies in on-line pré-concentration system for lead determination in drinking water and saline waste from oil refinery. Microchem. J. **77**, 123–129 (2004)
29. Khajeh, M.: Optimization of microwave-assisted extraction procedure for zinc and copper determination in food samples by Box–Behnken design. J. Food Compos. Anal. **22**, 343–346 (2009)
30. Montgomery, D.C.: Design and Analysis of Experiments. Wiley, Hoboken (2005)